Analysis, simulation, and experimental studies of YAG and CO_2 laser-produced plasma for EUV lithography sources

A. Hassanein, V. Sizyuk, S.S. Harilal, and T. Sizyuk
School of Nuclear Engineering and Center for Materials Under Extreme Environment
Purdue University, West Lafayette, IN 47907 USA

ABSTRACT

Efficient laser systems are essential for the realization of high volume manufacturing in extreme ultraviolet lithography (EUVL). Solid-state Nd:YAG lasers usually have lower efficiency and source suppliers are alternatively investigating the use of high power CO_2 laser systems. However, CO_2 laser-produced plasmas (LPP) have specific characteristics and features that should be taken into account when considering them as the light source for EUVL. The analysis of recent experimental and theoretical work showed significant differences in the properties of plasma plumes produced by CO_2 and the Nd:YAG lasers including EUV radiation emission, source formation, debris generation, and conversion efficiency. The much higher reflectivity of CO_2 laser from liquid, vapor, and plasma of a tin target results in the production of optically thinner plumes with higher velocity and in a better formation of plasma properties (temperature and density values) towards more efficient EUV source. However, the spikes in the temporal profiles of current CO_2 laser will additionally affect the properties of the produced plasma. We have developed unique combination of state-of-the art experimental facilities (CMUXE Laboratory) and advanced computer simulation (HEIGHTS) package for studying and optimizing various lasers, discharge produced plasmas (DPP), and target parameters as well as the optical collection system regarding EUV lithography. In this work, detailed characteristics of plasmas produced by CO_2 and Nd:YAG lasers were analyzed and compared both experimentally and theoretically for optimizing EUV from LPP sources. The details of lower overheating of plasma produced by CO_2 laser are given with time and explain how to utilize the high reflectivity of such lasers in plasmas produced in different target geometries to significantly enhance the conversion efficiency of EUV radiation.

Keywords: EUV, LPP, DPP, HEIGHTS, Debris mitigation, CO_2 Laser.

1. INTRODUCTION

Recent trends of analysis of the Extreme Ultraviolet Lithography (EUVL) community are directed toward improvement in the efficiency of laser-produced plasma (LPP) architecture with the CO_2 laser systems. Such systems have many advantages in comparison with Nd:YAG lasers. The optimal laser intensity for producing efficient EUV radiation output from Sn plasma generated by CO_2 laser corresponds to about 5×10^9 W/cm^2 [1], [2] while in the case of 1 μm wavelength Nd:AYG laser this intensity is around 5×10^{10} W/cm^2 [2], [3]. An order of magnitude less CO_2 laser power density is required for the production of efficient EUV source (for the same laser spot size). In addition, the possibility of using longer laser pulse [2], [4], lower droplets emission [5] and effects of laser wavelength on ionic and atomic emission from laser produced tin and lithium plasmas [6], [7] lead to more detailed investigations of plasma plumes produced by the CO_2 laser beams and to explore ways for improving the plasma optical properties for optimizing the EUV radiation emission.

We compared the characteristics of plasmas produced by CO_2 and Nd:YAG lasers using our HEIGHTS (High Energy Interaction with General Heterogeneous Target Systems) computer simulation package, which is continuously being upgraded and currently has numerous integrated models including 3-D laser energy deposition and target thermal response, surface melt-layer formation and movement, 3-D vapor and plasma magnetohydrodynamics, and 3-D photon line and continuum radiation transport with detailed library of atomic physics data for a number of candidate materials. Based on the various developed integrated models, HEIGHTS package allows to simulate the entire cycle of plasma generation, evolution, and interactions in LPP and DPP devices [3], [8], [9] starting from the initial solid target with any geometry in full 3-D configurations.

Extreme Ultraviolet (EUV) Lithography, edited by Bruno M. La Fontaine, Proc. of SPIE Vol. 7636,
76360A · © 2010 SPIE · CCC code: 0277-786X/10/$18 · doi: 10.1117/12.848222

2. CHARACTERISTICS OF PLASMA PLUMES PRODUCED BY Nd:YAG and CO_2 LASERS

Detail model description of the laser energy absorption and reflection, implemented in the HEIGHTS, is given in Ref. [3] with experimental parameters for the tin target. The Monte Carlo method recently developed for energy deposition in HEIGHTS allows considering in details the absorbed, reflected, reabsorbed, and transmitted photons, as well as the area in the plasma formation zone of the most intensive absorption and heating. Figures 1 and 2 illustrate distribution of absorbed energy of the CO_2 and Nd:YAG lasers, accumulated for the total time of the laser energy deposition with laser pulse width of 30 ns and 10 ns (FWHM) respectively. We chose the large spot size of 500 μm (FWHM) for both lasers with an intensity ~ 5×10^{10} W/cm^2 and comparatively long pulse duration in the case of CO_2 laser as these characteristics are preferred for producing the EUV radiation.

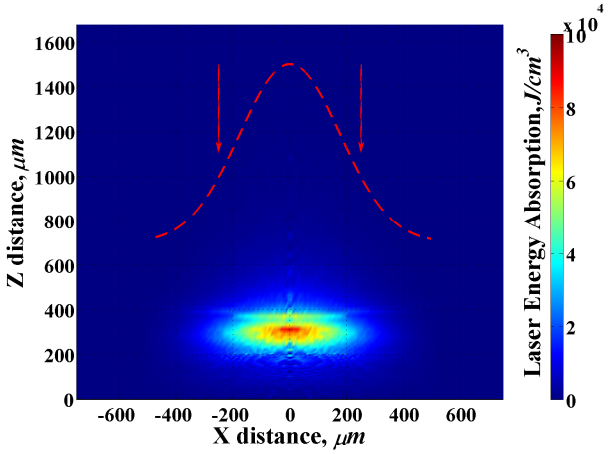

Fig.1. Spatial distribution of laser energy absorption for 10.6 μm laser wavelength accumulated in time

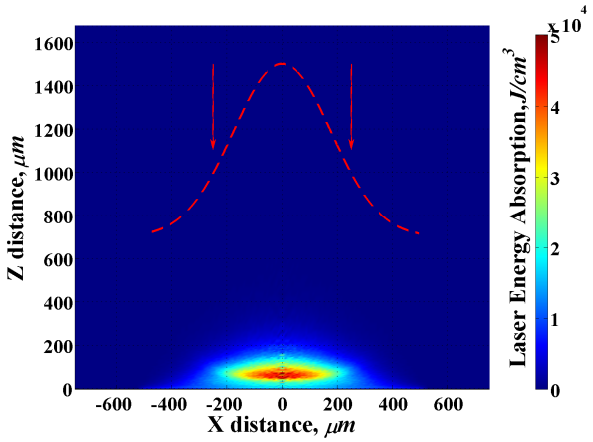

Fig.2. Spatial distribution of laser energy absorption for 1.06 μm laser wavelength accumulated in time

Due to the longer wavelength, the CO_2 laser radiation cannot penetrate deep into a dense plasma compared to Nd:YAG laser radiation because the reflection condition of radiation in plasma (radiation frequency approaches plasma frequency) can be satisfied much easier for the CO_2 laser waves [10]. The overheating effect of the plume peripheral areas is direct consequence of the CO_2 laser radiation properties. Preferential absorption of the CO_2 laser photons in the peripheral region with low plasma density causes increasing of the plasma temperature: the maximal electron temperatures exceed 100 eV for a laser intensity of 5×10^{10} W/cm^2, while in case of the Nd:YAG laser this value reaches only about 50 eV.

Previous studies showed that [2], [3] the optimal laser intensity for producing an efficient EUV source using 10.6 μm and 1.06 μm were $5\text{x}10^9$ W/cm^2 and $5\text{x}10^{10}$ W/cm^2 respectively and these parameters depended strongly on laser spot size [2], [3]. We compared the properties of Sn plasmas produced by 10.6 μm and 1.06 μm at these laser power density levels. Our calculations showed both the plasmas reach the same maximum temperature around 50 eV.

Lower absorption of the 10.6 μm laser waves in the dense matter (solid/liquid/vapor) and the less intensity of this laser beam required for the effective EUV output lead to decreasing of the ablation thickness and therefore, reducing the evaporated mass. The deposition and partition of the laser energy with more stronger absorption of the CO_2 laser radiation in the upper superficial region compared to Nd:YAG laser corresponds to the difference in the erosion profile of the tin target showed in Figure 3. The depth of erosion by the CO_2 laser is about 0.3 μm while in the case of Nd:YAG laser this value reaches about 1.1 μm. These results are for the optimum laser beam parameters described above.

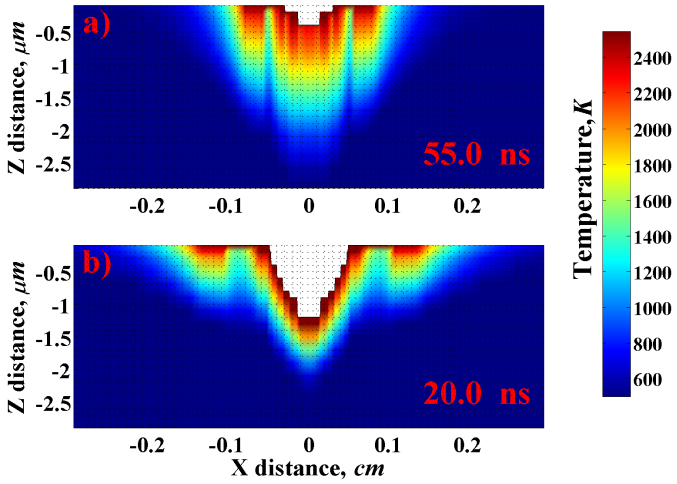

Fig.3. Erosion of tin target ablated by a) CO_2 laser with an intensity of $5x10^9$ W/cm^2 and b) Nd:YAG laser with an intensity of $5x10^{10}$ W/cm^2. Spot size is 500 μm in both cases.

Typically CO_2 laser beam has a long pulse length and complicated spiky shape [11] while the YAG laser in general possess Gaussian temporal profile. We analyzed the influence of the deposition time of the laser energy on the total EUV output in 2π solid angle with time. The intensity profiles in Figures 4 and 5 demonstrate the strong dependence of the EUV emission on the temporal profiles of CO_2 and Nd:YAG laser pulses.

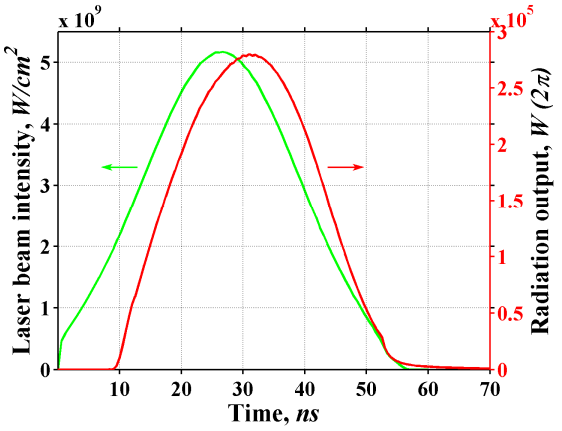

Fig.4. Time profile of laser beam intensity and EUV radiation output for 10.6 μm laser wavelength

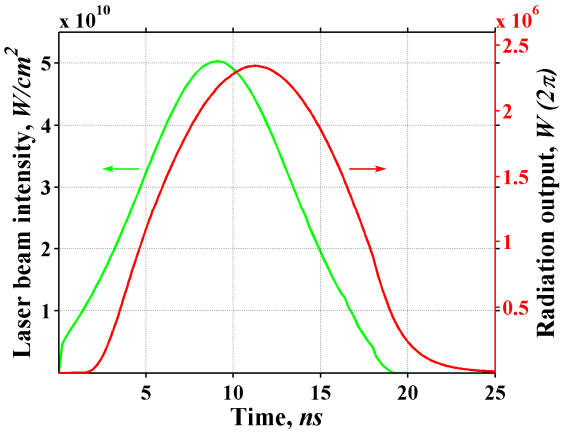

Fig.5. Time profile of laser beam intensity and EUV radiation output for 1.06 μm laser wavelength

In the case of 1.06 μm laser the EUV radiation output is quite longer than incident laser pulse width. This can be explained due to the chosen laser parameters in the modeling with a larger spot size (500 μm) and 10 ns (FWHM)

deposition time. This laser beam parameters produced and heated the tin plasma with sufficient mass and energy that led to more time for cooling of this plasma.

A special case with pulse profile typical for CO_2 lasers found in the experiment [2] and then implemented in our HEIGHTS modeling is shown in Figure 6. The complex temporal pulse shape of this laser significantly influences the time dependence of the EUV radiation output. The time dependence of the plasma temperature follows similar behavior with maximum values varied from 45 eV at 50 ns to 30 eV at 55 ns which influences the EUV radiation output. Figure also illustrates that an initial part of CO_2 typical pulse is inefficient for the EUV production.

The electron temperature and density distributions shown in Figures 7 and 8 demonstrate the difference in the plasma plume formation, where an order of magnitude lower density values in the case of CO_2 laser achieves the same temperatures as the Nd:YAG laser with the higher intensity. The higher plasma density will follow the cooling inertia in the Nd:YAG produced plasmas and therefore, can explain the longer delay in the time profile in Fig. 5 between the laser power and the EUV radiation output.

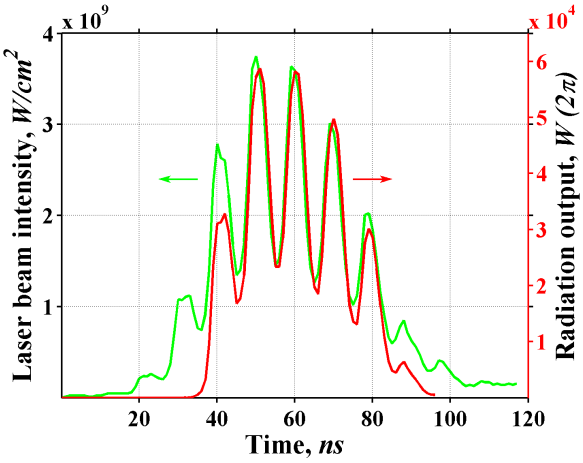

Fig.6. Experimental time profile of laser beam intensity and modeled EUV radiation output for 10.6 μm laser wavelength

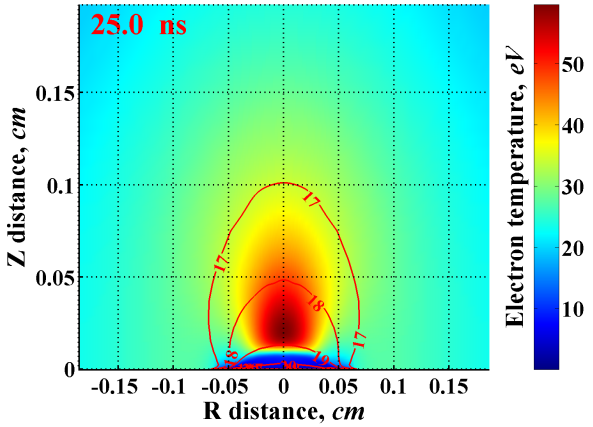

Fig.7. Electron temperature and density (red contours) distribution in plasma plume produced by CO_2 laser with intensity of $5x10^9$ W/cm^2

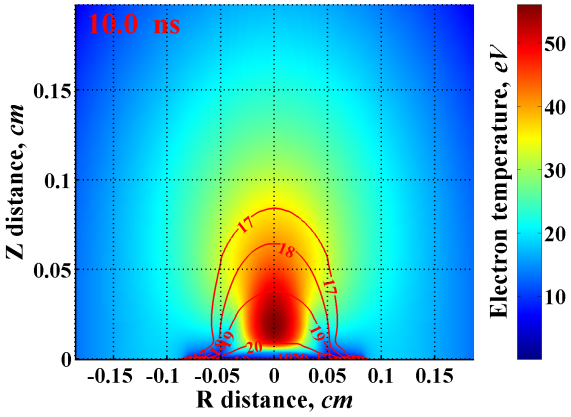

Fig.8. Electron temperature and density (red contours) distribution in plasma plume produced by Nd:YAG laser with intensity of $5x10^{10}$ W/cm^2

The same difference in values of density distribution was observed in the experiments performed in our CMUXE laboratory. Figure 9 shows electron density at the peak of laser energy impact for Nd:YAG and CO_2 lasers with parameters similar to our calculations. The density plots were obtained using a Nomarski interferometer employing frequency doubled YAG laser (5 ns FWHM) as the probe beam [2]. Plasma produced by 1.06 μm wavelength has electron densities with higher gradient near the target and shows maximum value of $5x10^{20}$ cm^{-3} at 100 μm from the surface, while 10.6 μm laser produces plasma with maximum electron density around $5x10^{19}$ cm^{-3}.

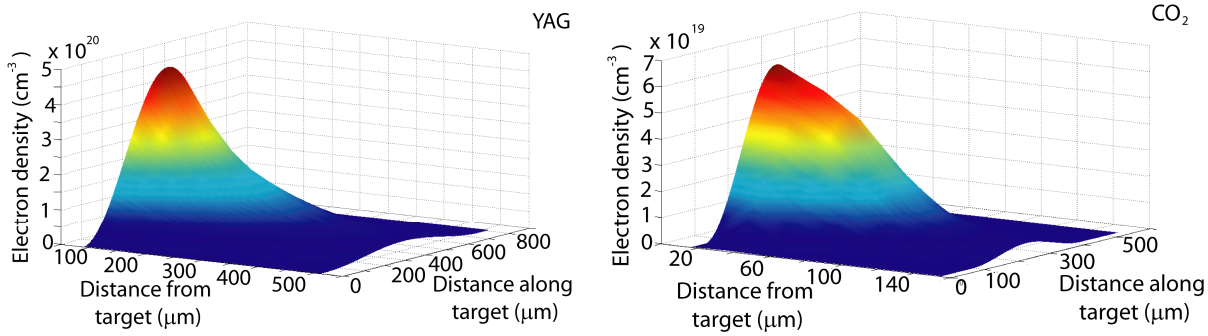

Fig.9. Electron density distribution in plasma plume produced by Nd:YAG laser and CO_2 laser measured using Nomarski interferometry

We utilized the HEIGHTS Monte Carlo model for detailed radiation transport simulation which calculates the location and intensity of the photon source for EUV output in 2π sr. The combinations of electron density and temperature distributions explain difference in the location of the maximum EUV photons emission and absorption, and intensity of EUV radiation fluxes (Figures 10 and 11).

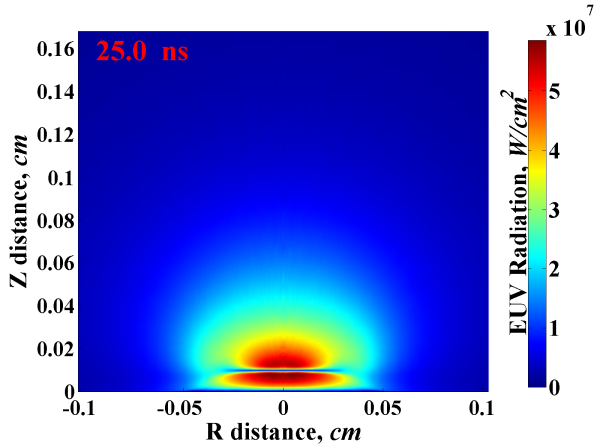

Fig.10. EUV radiation fluxes in tin plasma produced by CO_2 laser at the peak of laser energy impact

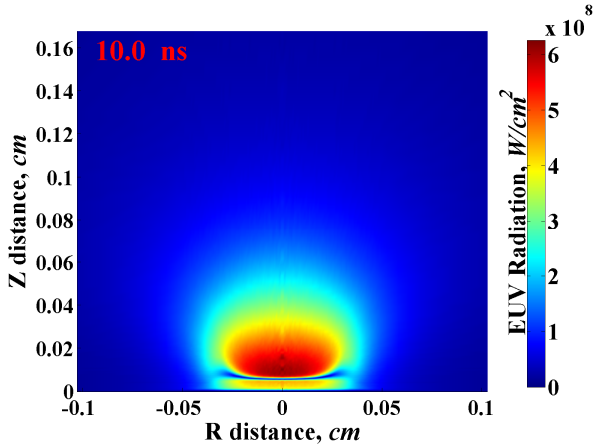

Fig.11. EUV radiation fluxes in tin plasma produced by Nd:YAG laser at the peak of laser energy impact

Figures 12 and 13 illustrate the source of EUV photons emitted at the peak of the laser pulse for CO_2 and YAG lasers. The density and temperature determine the location and the intensity of the EUV source output in 2π sr, where maximum EUV photons, reached the optical collection mirror system, is produced in area with a range of electron densities around 10^{19} cm^{-3} for CO_2 laser and 10^{20} cm^{-3} for Nd:YAG laser as shown in Figures 12 and 13 respectively.

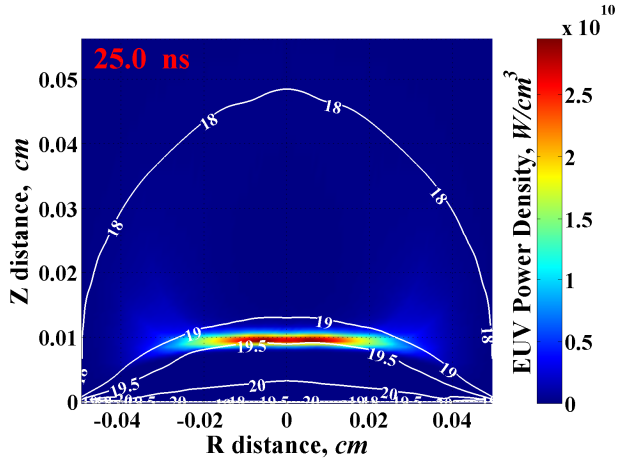

Fig.12. Source of EUV radiation in the correspondence with the electron density (white contours) in system with CO_2 laser

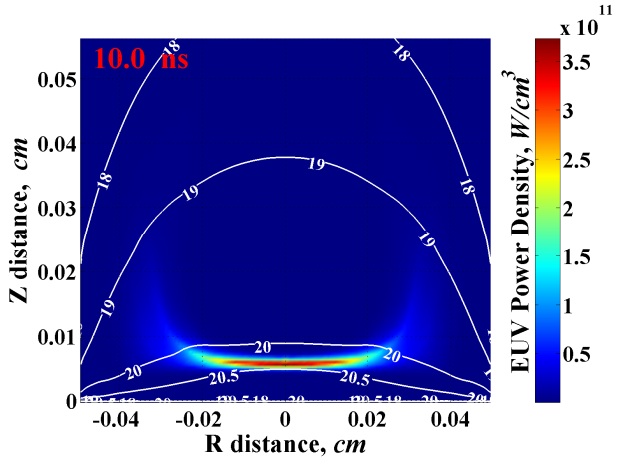

Fig.13. Source of EUV radiation in the correspondence with the electron density (white contours) in system with Nd:YAG laser

The dependence of the laser wavelength on tin mass ablation slightly influences the angular distribution of the EUV radiation output. Figure 14 shows the difference in EUV radiation emission as a function of the angle with respect to target normal at the peak of the laser beam intensity for Nd:YAG and CO_2 lasers. The EUV emission from Nd:YAG LPP showed slightly larger decay with target normal compared to CO_2 LPP. The presence of cold dense plasma lobes at angles 45° with respect to target normal for the 1.06 μm LPP (Fig. 8) absorbs EUV photons. Also with increasing the pulse length of the laser, a drastic change in angular dependence of EUV output can be detected for Nd:YAG laser. In the case of CO_2 laser beam, the decrease in laser radiation absorption leads to a reduced evaporation and reduced mass inflow into the 45° angle observation region. As a result, the EUV absorption is considerably reduced at higher angles.

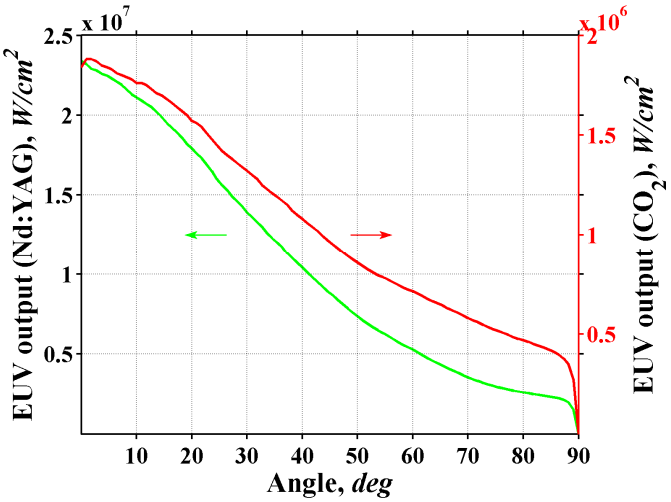

Fig.14. Angular distribution of EUV radiation output from Sn plasma produced by Nd:YAG (green plot) and CO_2 (red plot) lasers

CONCLUSION

We investigated the wavelength effects of the laser light on the temporal and spatial features of the EUV radiation emission from laser-produced Sn plasmas. For this analysis we utilized a unique combination of experimental studies at our CMUXE laboratory and our advanced computer simulation (HEIGHTS) package. Detailed characteristics of plasmas produced by CO_2 and Nd:YAG lasers showed substantial differences in basic plasma properties. Our calculations showed, for example, that the Sn target erosion is nearly an order of magnitude less for plasmas produced by 10.6 μm compared to 1.06 μm radiation. Similarly the calculated density of the 1.06 μm produced plasma is found to be an order higher compared to CO_2 LPP which are consistent with measured values in our CMUXE experiments using

interferometry technique. Though both the plasmas produced by CO_2 and YAG laser showed same peak temperature, the Nd:YAG plasmas showed slightly more angular dependence on the EUV radiation emission.

ACKNOWLEDGEMENT

Major part of this work is supported by Purdue University, College of Engineering.

REFERENCES

[1] Fomenkov, I. V., Brandt, D. C., Bykanov, A. V., Ershov, A. I., Partlo, W. N., Myers, D. W., Böwering, N. R., Farrar, N. R., Vaschenko, G. O., Khodykin, O. V., Hoffman, J. R., Chrobak, C. P., Srivastava, S. N., Golich, D. J., Vidusek, D. A., De Dea, D., and Hou, R. R., "Laser-Produced Plasma Light Source for EUVL", Emerging Lithographic Technologies XII, Proc. of SPIE **7271-38** (2009).

[2] Harilal, S. S., Coons, R. W., Hough, P., and Hassanein, A., "Influence of spot size on extreme ultraviolet efficiency of laser-produced Sn plasmas," Applied Physics Letters **95,** 221501 (2009).

[3] Hassanein, A., Sizyuk, V., Sizyuk, T., and Harilal, S. S., "Effects of Plasma Spatial Profile on Conversion efficiency of Laser-Produced Plasma Sources for EUV lithography," J. Micro/Nanolith. MEMS MOEMS **8,** 041503 (2009).

[4] Tao, Y., Tillack, M. S., Sequoia, K. L., Burdt, R. A., Yuspeh, S., and Najmabadi, F., "Efficient 13.5 nm extreme ultraviolet emission from Sn plasma irradiated by a long CO2 laser pulse," Applied Physics Letters **92,** 251501 (2008).

[5] Takahashi, A., Nakamura, D., Tamaru, A., Akiyama, T., and Okada, T., "Comparative study on EUV and debris emission from CO2 and Nd: YAG laser-produced tin plasmas," Journal of Physics: Conference Series **112,** 042059 (2008).

[6] Campos, D., Coons, R. W., Fields, M. D., Crank, M., Harilal, S. S., and Hassanein, A., "Angular distribution of debris from CO_2 and YAG laser-produced tin plasmas", these proceedings.

[7] Coons, R. W., Campos, D., Crank, M., Harilal, S. S., and Hassanein, A., "Comparison of EUV spectral and ion emission features from laser-produced Sn and Li plasmas", these proceedings.

[8] Hassanein, A., Sizyuk, V., and Sizyuk, T., "Multidimensional simulation and optimization of hybrid laser and discharge plasma devices for EUV lithography," Proc. of SPIE **6921,** 92113 (2008).

[9] Sizyuk, V., Hassanein, A., Morozov, V., Tolkach, V., Sizyuk, T., and Rice, B., "Numerical simulation of laser-produced plasma devices for EUV lithography using the heights integrated model," Numerical Heat Transfer Part a-Applications **49,** 215-236 (2006).

[10] Johnston, T. W., and Dawson, J. M., "Correct values for high-frequency power absorption by inverse bremsstrahlung in plasmas," Phys. Fluids **16,** 722 (1973).

[11] Hurst, N., and Harilal, S. S., "Pulse shaping of transversely excited atmospheric CO2 laser using a simple plasma shutter," Review of Scientific Instrumentation **80,** 035101 (2009).